J Solid State Electrochem (2012) 16:603–615
DOI 10.1007/s10008-011-1391-y

ORIGINAL PAPER

GBL-based electrolyte for Li-ion battery: thermal and electrochemical performance

Dmitry Belov · Deng-Tswen Shieh

Received: 26 January 2011 / Revised: 20 March 2011 / Accepted: 30 March 2011 / Published online: 20 April 2011

Abstract Thermal stability, flammability, and electrochemical performances of the cyclic carbonate-based electrolytes [where γ-butyrolactone (GBL) is a main component (at least 50 vol.%) among of EC and PC with $LiBF_4$] have been examined in comparison with contemporary (EC/EMC, 1:3 vol.%, 1 M $LiPF_6$) electrolyte by DSC, accelerating rate calorimetry (ARC), AC impedance, and cyclic voltammetry (CV). This study shows that GBL-based electrolytes have perfect thermal stability and will improve Li-ion battery safety (including flammability) without performance trade-off with the accurate combination of active materials and separator. Several types of negative electrode materials (such as hard carbon, MCMB, and SWF) have been tested to evaluate GBL-based electrolyte influence on SEI formation and battery performance. Finally, GBL-based electrolytes show not only equal electrochemical performance in comparison to commonly used electrolytes (EC/EMC in this study) but it will notably improve battery safety.

Keywords Li-ion battery · Gamma butyrolactone · Non-flammable · Thermal stability · Safety

Introduction

Despite all the attractiveness and versatility of Li-ion batteries, they have one serious weakness, and that is safety. It is obvious that when increasing a battery's energy density, the safety concern becomes more critical. This has been clearly displayed over the recent years when the frequency and the volume of the battery recalls due to potential safety risk have been expanded. In the past years, a number of attempts have been made to comprehend and model Li-ion battery's thermal behavior [1, 2] and safety [3] to improve its design and reliability. However, the Li-ion battery is a multi-component system, and its modeling in terms of safety is a very complicated multi-task. Cell design and materials combination become the crucial factors for battery safety. Combination of highly reactive (at fully lithiated state) carbon, a soft and thin polyolefin (PO) separator film, and highly flammable and reactive electrolytes (for example, the flash point of DEC is 31 °C and EMC is only 22.5 °C) makes Li-ion battery thermally unstable when one of the components fails.

Previously [4], we have demonstrated that thermal runaway of Li-ion battery significantly affected by electrically conducting dendrites growing inside the separator during charge. Thus, PO separator film and highly flammable electrolytes are the battery's most critical elements (in terms of safety) that have no real alternatives for replacement at this moment. The approaches to enhance Li-ion battery safety with electrolyte (overcharge) additives have been discussed elsewhere [5], and they are mostly ineffective and have a lot of limitations [6].

Electrolytes for Li-ion batteries used in electric vehicles (EVs) (HEV, PEV, etc.) and energy storage systems have some specific requirements (above a line of fundamentals such as high/low temperature operation range, high ionic conductivity, considerably stable to positive/negative materials, i.e., wide electrochemical window, and chemical inertness to all battery components). It must be safe: high thermal

D. Belov (✉) · D.-T. Shieh
Industrial Technology Research Institute (ITRI),
Bldg. 77, 195, Sec. 4, Chung Hsing Rd.,
Hsinchu 31040, Taiwan
e-mail: dmitry@belovs.info

stability at elevated temperatures during rapid charge/discharge (vehicle acceleration/breaking), non-flammable, and have a long cycle/calendar life. One of the approaches to enhance Li-ion battery safety is to use inherently safe electrolyte solutions, for example, room temperature ionic liquids (RTIL) [7, 8] or electrolyte solvents with high boiling and flash points (such as aprotic polar solvents), which are safer but less practical due to its high viscosity and lower ionic conductivity. Development of the thermally and chemically stable Li salts (pure $LiPF_6$ salt is thermally stable up to 107 °C in a dry inert atmosphere [9] and <80 °C in EC/DMC) is another approach to improve Li-ion battery safety. However, RTILs require deeper study for its application in Li-ion batteries (in general, due to the formation of an unstable SEI layer by the reductive decomposition of the RTIL at low potential, which restricts the application of ionic liquids today). Cyclic carbonates such as ethylene carbonate (EC) are a solid at the room temperature and propylene carbonate (PC) exfoliate most of the carbonaceous materials, and it decomposes when in contact with graphitized carbon at potentials less than 1 V versus Li/Li^+. Among them, GBL possesses a high boiling and flash temperature (T_m=−43 °C; T_b=204 °C; T_f=97 °C) but show relatively low viscosity (1.73 cP at 25 °C), good ionic conductivity, and have a high dielectric constant (e=39). The last one allows it to dissolve most of the Li salts [including highly thermally stable Li salts such as lithium bis-oxalatoborate (LiBOB) and bis (trifluoromethane sulfonyl) imide (LiTFSI)] to sufficient concentrations very easily. It has been shown that GBL-based electrolytes can be successfully used in Li-ion batteries in a large range of temperatures [10, 11]. As well as an additive to common electrolytes, it can depress gassing generated by EC decomposition [12, 13]. Finally, it also can act as a stabilizing component for the Al foil even in a solution containing the highly corrosive salt LiTFSI [14].

In this study, we will focus on the investigation of the (a) thermal stability (and flammability) of the GBL-based electrolyte in correlation with conventional electrolytes (by DSC and ARC technique and burning test), (b) electrolyte composition optimization (salt type, ionic conductivity, McMullin number), and (c) electrochemical performances of the GBL-based electrolytes in combination with different types of negative electrodes.

Experimental

Materials

Electrolyte components such as ethylene carbonate (EC), propylene carbonate (PC), γ-butyrolactone (GBL), vinylene carbonate (VC) as additive, $LiBF_4$ (battery grade), and EC/EMC (1:2, v/v), 1 M $LiPF_6$ with 2 wt.% VC were purchased from Ferro and used as received. LiBOB (premium battery grade, purity 99.99%) was kindly provided by Chemetall (Frankfurt) as a free sample. $LiN(SO_2C_2F_5)_2$ was purchased from 3M (Minneapolis, MN, USA).

Separators DSM "Solupor" [polyethylene (PE)], Celgard 2400 [polypropylene (PP)], Celgard 2320 (PP/PE/PP), and Asahi ND416 (PE) were used (more details of separator properties in Table 1).

Sample preparation

Negative electrode (NE) was made with MCMB 1028, SWF 15P10, and hard carbon P(J) with PVDF or acrylic binder (in case of SWF) on copper foil (14 μm). Positive electrode (PE) was made with $Li(Ni_{0.8}Co_{0.15}Al_{0.05})O_2$ (LNCA) with a PVDF binder on aluminum current collector (20 μm). All electrodes were made with a small coater (CHIBI coater with drying oven) with a standard procedure of mixing and coating. All electrode materials were dried at 150 °C in a vacuum oven for 6 h before the cell assembly.

All samples of electrolyte solution have been prepared in a glove box under an argon atmosphere (electrolyte compositions are listed in Table 2); coin cell (CR2032), Al-laminated bag (single cell), and prismatic jellyroll cells

Table 1 Separator characteristics and McMullin number

Separator	Polymer type	Impregnation rate[a]	Process	Thickness (μm)	Porosity (%)	McMullin number[b]	
						EMC	GBL2
Asahi ND416	PE	Fast	Wet	16	43	13	7
Celgard 2320	PP/PE/PP	Very slow	Dry	20	39	15	7.9
Celgard 2400	PP	Slow	Dry	25	37	8.9	9.8
DSM "Solupor"	PE	Very fast	Wet (gel technology)	16	42	25	27

[a] Fast < 0.5 min > slow

[b] Calculated by using electrolyte conductivity of "EMC" and "GBL2" from Table 3

Table 2 Electrolyte compositions and its conductivity (at 20 °C in dry room environments, dew point is −45; all samples have 2 wt.% VC)

Solvent/salt	Flash point (°C)	Volume %					
		Short code					
		EC/EMC	EC/EMC	GBL1	GBL2	GBL3	GBL4
EC	143	50	32	50	40	40	30
PC	132				10	20	20
GBL	97	50		50	50	40	50
EMC	22		68				
VC	73			Molar concentration, M			
$LiBF_4$		1		1.5	1.4	1.4	1.4
$LiPF_6$			1				
Conductivity (mS cm^{-2})							
Conductivity		2.1	9.05	6.14	6.0	5.63	5.48
Viscosity, cP (25 °C)	2.78	–	3.86	–	–		

were assembled in a dry room atmosphere. Al-laminated bag with prismatic jellyroll electrodes were assembled as SWF/DSM/LNCA (full cell) for three-electrode study and charge/discharge tests with a nominal capacity of 375 mAh.

Electrochemical tests and thermal performance measurements

Electrolyte conductivity measurements were done by WTW/Cond 330i/SET (Germany) with GC electrodes, and AC impedance measurement has been done with the Solartron 1255B (Frequency Response Analyzer) with a SI1287 (Electrochemical Interface). In the EIS measurements, a frequency range was set from 1 MHz to 0.1 Hz, and the test amplitude of the EIS was 10 mV. Cyclic voltammetry (CV) has been done with a MacPile II cycler connected to a Power Macintosh 7200/120 with MacPile software. The scan rate of CV measurements was 0.05 mV s^{-1}. Charge/discharge characteristics and cycle ability of the cells were investigated with the Bitrode battery tester.

As a criterion to judge separator/electrolyte affinity and indirect measurement of the separator wet ability, the McMullin number has been used. The McMullin number is the value of the ionic conductivity of the electrolyte solution (measured by a conductivity meter) (C_{el}) divided by the ionic conductivity when the polyolefin membrane is impregnated with the electrolyte solution (C_{sep+el}). The last one was determined by measuring AC impedance at 10 kHz of a specimen sandwiched between two stainless steel plates with a diameter of 1 cm. Consequently, the smaller the McMullin number the better the wet ability and ionic conductivity of the separator.

Thermal properties of the electrolyte have been tested with DSC (Perkin Elmer) in high-pressure gold plated stainless steel pans. In accelerated rate calorimetry (ARC) (Thermal Hazard Technology, UK) measurements, 2.5 g of electrolyte solution was loaded in a titanium spherical sample holder (8 ml volume) (denoted as Ti-bomb) in an argon-filled glove box. Samples were heated from 50 to 350 °C in 5 °C increments (sensitivity threshold was 0.02 °C min^{-1}) with heat-wait-seek mode.

Results and discussion

Thermal stability and flammability tests

It is known that cyclic carbonates (such as EC, PC, and GBL) used as electrolytes for Li-ion battery have a higher thermal stability if compared with linear carbonates based on their general physical properties such as boiling and flash point. However, their thermal stability in activated Li-ion batteries has been studied considerably less than their counterparts [electrolyte mixes of EC (PC) and one of linear carbonates such as EMC, DMC, DEC, etc.]. Furthermore, every composition of the electrolyte (solvent ratio and salt type/concentration) will exhibit different inherent characteristics as well as cell performance. In this part, we first study the thermal stability of electrolytes with compositions as (1) EC/GBL (1:1, v/v) 1.5 M $LiBF_4$ (denoted as GBL1) and (2) EC/EMC (1:2, v/v) 1 M $LiPF_6$ (denoted as EC/EMC) as a reference and widely used electrolyte (details in Table 2) by DSC technique. VC (2 wt.%) was added in each electrolyte as a vital solid electrolyte interface (SEI) enhancer additive and due to its relatively low flash point (73 °C) compared to other electrolyte components. The reason we have used those two electrolytes for our further experiments on thermal study but not "equal" systems such as EC/EMC, $LiBF_4$ or EC/

GBL, $LiPF_6$, i.e., composition with different solvents but equal salt, is quite obvious. Both above-mentioned electrolytes are practically useless. The first one has too small ionic conductivity (as seen from Table 2) and the second one has no ability for reversible lithium intercalation [as discussed below in "Electrochemical performance: ionic conductivity (salt and solvent composition)" section], which makes comparison of such electrolytes meaningless (at least from practical point of view). The results of DSC analysis of these electrolytes are illustrated in Fig. 1. Reference electrolyte (EC/EMC) decomposition indicates the main exothermic peak (Fig. 1, curve a) with onset temperature at 225 °C and maximum temperature at about 270 °C (ΔH=184 J g^{-1}). A small endothermic peak at 245 °C corresponds to the reaction between the salt ($LiPF_6$) and the EMC as have been shown by Botte et al. [15]. For the GBL1 electrolyte (Fig. 1, curve b), onset temperature shifted to 290 °C with a maximum of the electrolyte decomposition temperature at 340 °C (ΔH=375 J g^{-1}). No endothermic reaction between Li salt ($LiBF_4$) and electrolyte solution has been observed. However, there is a small exothermic peak at about 200 °C, which may be attributed to the $LiBF_4$ decomposition [16].

Moreover, a DSC test of the de-lithiated LNCA electrode with the above-mentioned electrolytes has been performed to evaluate the thermal stability of the electrolytes with an active material. Samples have been prepared by cycling of coin cells (LNCA/separator/Li, half cell) up to five times with a low current (C/5) to 4.2 V. After coin cells are dismantled in an argon glove box, about 10 mg of LNCA/binder/electrolyte powder was carefully transferred to the high-pressure DSC pan. The results are shown in Fig. 2. There are two exothermic peaks for the sample of LNCA with the EC/EMC electrolyte (Fig. 2, curve a). The first broad peak has a maximum at about 225 °C and second (main) sharp peak at 243 °C due to the interfacial reaction of de-lithiated LNCA with liquid electrolytes. Onset temperature starts at 180 °C

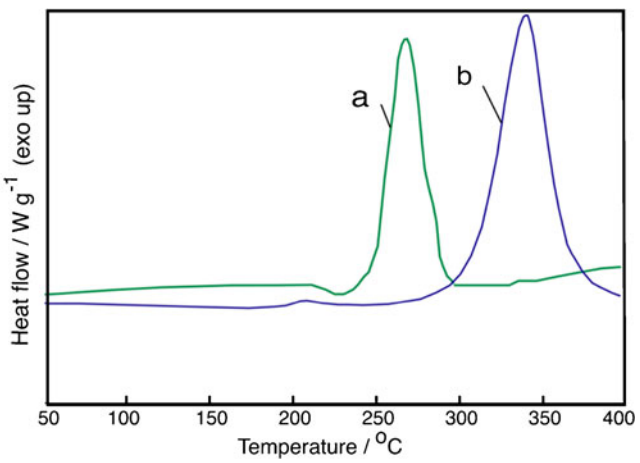

Fig. 1 DSC curves of *a* EC/EMC (1:2), 1 M $LiPF_6$ and *b* EC/GBL (1:1), 1.5 M $LiBF_4$ electrolytes. Scan rate 10 °C min^{-1}

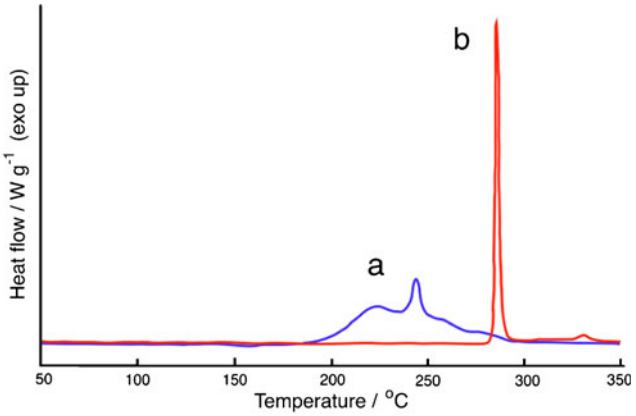

Fig. 2 DSC curves of the fully de-lithiated cathode (LNCA, cut-off at 4.2 V vs. Li^+/Li) electrode with (1) EC/EMC (1:2), 1 M $LiPF_6$ and (2) EC/GBL (1:1), 1.5 M $LiBF_4$ electrolyte. Scan rate 10 °C min^{-1}

with total heat generation of 883 J g^{-1}. For GBL-based electrolyte, there is only one sharp peak (Fig. 2, curve b) with a maximum temperature at 285 °C and total heat generation is 583 J g^{-1}. A small peak at 335 °C may be attributed to electrolyte decomposition as shown above (Fig. 1). These DSC test results clearly show that GBL-based electrolyte with $LiBF_4$ salt has significantly enhanced thermal stability at wide high temperature range even in the presence of a fully lithiated positive electrode material. Such effect of thermal stability might also be a synergy effect between a high boiling point solvent and highly thermally stable $LiBF_4$ salt [17].

For flammability tests, we have used a laboratory gas burner and Petri dishes (∅50 mm) filled with 10 g of electrolytes (as in DSC test). It was revealed that EC/EMC electrolyte catches fire immediately and after the self-burning process was finished (in a few minutes) the total weight loss of electrolyte became 56%. On the contrary, the GBL1 electrolyte has no flame during about a minute of burning and no weight loss (Fig. 3). So far there is no clear definition of the non-aqueous electrolyte flammability (non-

Fig. 3 Burning test, EC/GBL, 1:1, 1.5 M $LiBF_4$ electrolyte under laboratory gas burner

flammability) terms, and according to PTCL Safety Glossary (Physical and Theoretical Chemistry Laboratory, Oxford University) [18], "a nonflammable material is one, which cannot be ignited (although the term is sometimes also used to indicate a material which, while it can be ignited with difficulty, burns only very slowly)"; it is possible to classify GBL and GBL-based electrolytes as "nonflammable".

Although DSC tests will show a material's thermal properties (physical and/or chemical transformation) and stability in a very precise way, the technique used quite a small amount of the substances and linear temperature ramp that make it difficult to simulate real battery environments, especially in terms of safety. The accelerated rate calorimetry (ARC) technique allows the simultaneous measurement of temperature and pressure of the separate or mixture of substances, and its intermediates in adiabatic conditions. The combination of the ARC test data (such as heat generation rate, onset and decomposition temperature, pressure generation and time to maximum rate, and temperature of no return/self-accelerated decomposition) provides close to real condition overview of the processes in the Li-ion battery and its components.

The ARC test data have been recorded as electrolyte temperature and pressure vs. time (Fig. 4) in the temperature range from 50 °C to 350 °C for two kinds of electrolyte solutions: EC/EMC (Fig. 4, curves a, c) and GBL2 (see Table 1) (Fig. 4, curves b, d). The pressure onset for EC/EMC electrolyte started at 110 °C and reached its first short maximum peak at 75 bar (with the maximum at 100 bar at the end of the test) (Fig. 4, curve a) when sample temperature reached to 165 °C (Fig. 4, curve c) and rapid exothermic reaction had been observed.

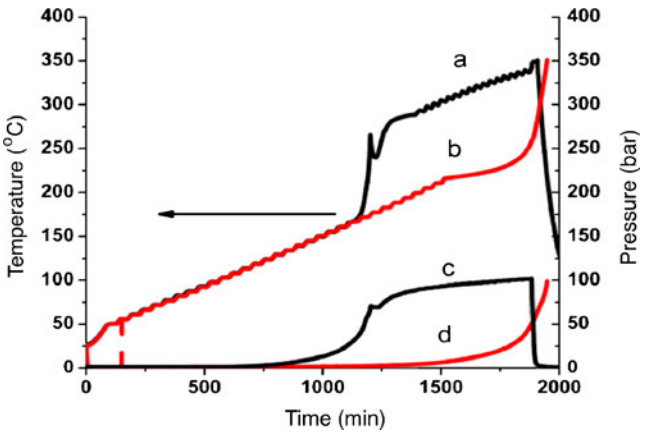

Fig. 4 ARC test of EC/EMC, 1 M $LiPF_6$ (*a* temperature; *c* pressure vs. time) and EC/PC/GBL, 1.4 M $LiBF_4$ (*b* temperature; *d* pressure vs. time)

After the temperature reached 270 °C, it failed shortly due to the inability of the ARC to record the data correctly (temperature rate is too high). When the temperature inside the ARC chamber reached ~340 °C, the pressure of the sample was about 100 bar and the EMC-based electrolyte blew up inside the Ti-bomb and totally destroyed it as seen in Fig. 5.

On the contrary, in the GBL-based electrolyte a heat-wait-seek mode continues to 216 °C (Fig. 4, curve b) and reveals an almost flat plateau (T–t curve) of self-heating process within 5 h (test time from 1,500 to 1,800 min), while pressure increases steadily from 5 to 27 bar only (Fig. 4, curve d) and reached its maximum of 100 bar when the temperature attained 350 °C (end point of test setting). After the tests, the sample holder (Ti-bomb) did not indicate any visual distortions and at the repeated tests exhibit identical results (can be re-used).

Figure 6 shows the equivalent data as on Fig. 4 and it is represented as log dT/dt vs. T and demonstrated self-heating rate for two electrolytes during the ARC test. The principal difference here is that self-heating rate for GBL-based electrolyte (Fig. 6, curve b) during the test will reach no more than 1.2 °C min^{-1} and become steady at temperatures below 300 °C until the test reached the program limitation temperature of 350 °C. Oppositely, EC/EMC electrolyte displays two self-heating peaks (Fig. 6, curve a) where the first one starts at 165 °C with a maximum heat rate of 1.2 °C min^{-1} (which may be attributed to $LiPF_6$ reactivity in the EC/EMC solvent) and the second reached maximum heat rate over 10 °Cmin^{-1} at 250 °C when Ti-bomb was destroyed.

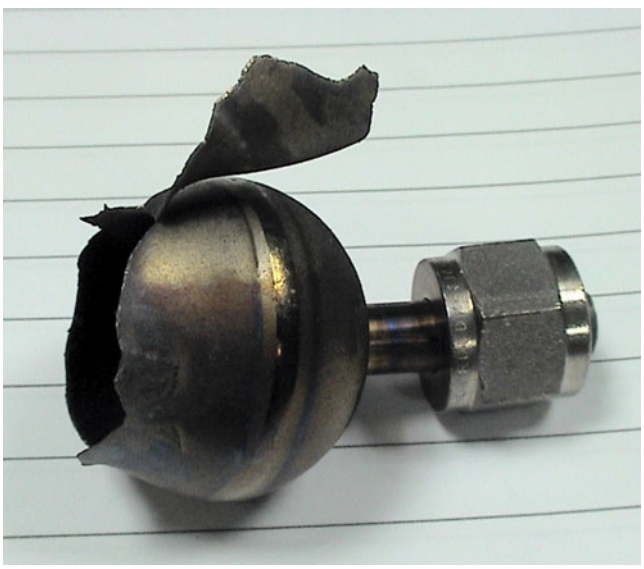

Fig. 5 Ti-bomb after ARC test with EC/EMC, 1:2, 1 M $LiPF_6$ electrolyte

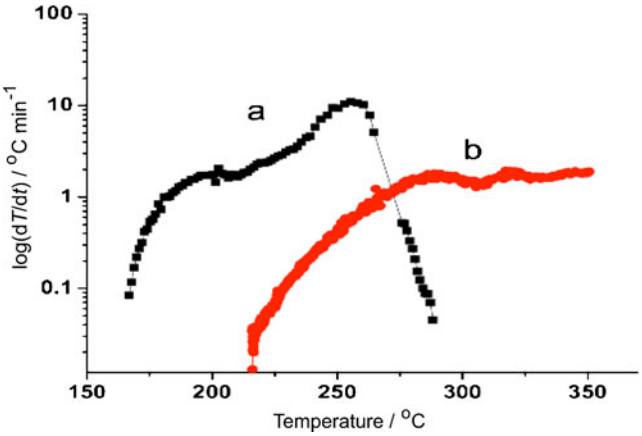

Fig. 6 ARC test as self-heating rate vs. temperature for 2.5 g electrolyte samples *a* EC/EMC, 1 M $LiPF_6$ and *b* EC/PC/GBL, 1.4 M $LiBF_4$

These tests clearly indicate that thermal stability of the GBL-based electrolytes with $LiBF_4$ salt is greatly higher in contrast to common electrolytes (mix of linear carbonates).

Furthermore, GBL-based electrolytes are overperforming in terms of thermal stability of most of the commonly studied ionic liquid electrolytes. It has been shown by Wang et al. [19] that some ionic liquids (such as EMI-FSI, EMI-TFSI, and Py13-FSI) are not even safer than commonly used electrolytes (EC, DEC 1 M $LiPF_6$). However, electrochemical performances of the GBL-based electrolytes are much stable and predictable compared to ionic liquid electrolytes, which will be shown further.

Electrochemical performance: ionic conductivity (salt and solvent composition)

Due to the excellent thermal stability of the GBL-based electrolytes as shown above (over conventional electrolyte systems and modern ionic liquids), its significant low cost and considerably lower viscosity compared to ionic liquids allowed us to consider replacing the highly flammable (linear carbonates) electrolyte components in Li-ion batteries and particularly in batteries for high power applications. However, there is not much information on the GBL-based electrolyte compatibility with various active materials (either positive or negative), separators, and its cycle ability at different conditions except for the few referred above and reviewed in [20]. Therefore, it is necessary to understand its compatibility and behavior with common (up to date) active materials and optimize electrolyte/salt(s)/additive(s) compositions as well as battery design to reach a safety/performance balance in equal conditions. Here, we present some of our studies.

For Li-ion battery (not considering of electrode material type and battery design here), the main factors limiting cell performance (such as a cycle and rate ability, calendar life, and safety) are mainly related to (a) electrolyte ionic conductivity, (b) electrolyte/separator wet ability (McMullin number), and (c) low/high temperature performance.

Table 3 Electrolyte conductivity (mS cm^{-2}) of the electrolytes with different Li salts in GBL (at 20 °C)

Li salt	Li salt concentration	
	1.0 M	1.2 M
$LiBF_4$	7.55	7.25
LiBOB	7.35	6.83
LiTFSI	9.24	

The ionic conductivity of the three Li salts with concentrations as 1 M and 1.2 M in pure GBL solvent has been tested, and the results are listed in Table 2. According to Chagnes et al. [21], $LiBF_4$ salt is the best choice for GBL-based electrolyte as it leads to the formation of a stable and high quality passivative layer in comparison to $LiPF_6$, which generated insulating phosphorous compounds toward Li-ions. The choice of LiBOB and LITFSI salts for this screening experiment is related to a known fact that they have an improved thermal stability and non-HF-generated compounds [22–24]. LiBOB has a great potential for use in lithium batteries due to its low degree of ion association, higher chemical/electrochemical stability, and absence of halogen atoms [25]. Additionally, highly corrosive salt LiTFSI in combination with GBL solvent can act as a stabilizing component for Al anode. The ionic conductivity of the electrolytes is slightly decreased with the increase of salt concentration from 1 M to 1.2 M that reflects the combined effect of salt solubility and solution viscosity. More notably, it is seen for electrolytes with LiBOB salt. To recognize the electrolyte cycle ability and avoid SEI formation effect on this stage of

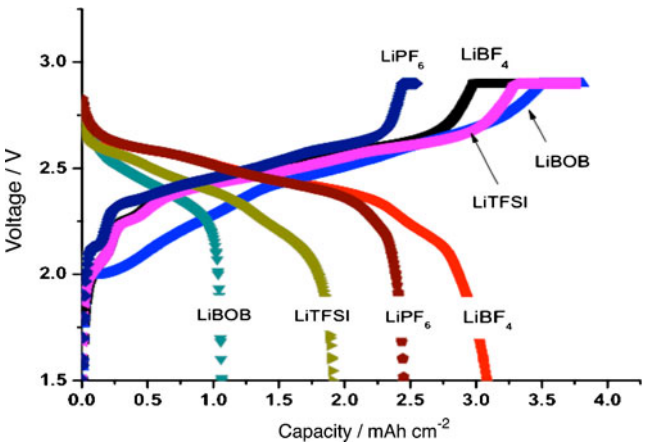

Fig. 7 First charge–discharge curves of $Li_4Ti_5O_{12}$/LNCM coin cells; 1 M of LiBOB, LiTFSI, and $LiBF_4$ in GBL; 1 M $LiPF_6$ in EC/EMC (as reference)

study, we have used $Li_4Ti_5O_{12}$ and LNCM as negative and positive electrodes in combination with electrolytes listed in Table 3. The sample cells were subjected to formation cycles at C/5 between 2.8 and 1.5 V. Figure 7 is a summary of the first cycle for four cells where a poor cycle ability of the LiBOB and LITFSI in pure GBL electrolyte is demonstrated. The coulombic efficiency of the sample cells with $LiBF_4$ salt is 92%, LiTFSI—76%, LiBOB—16%, and cell with reference electrolyte—96%. In other words, the ability of the tested Li salts for reversible Li intercalation/deintercalation in the presence of GBL-based electrolytes is as follows: $LiBF_4$> LiTFSI > LiBOB. It can be seen here that electrolyte conductivity value is not a clear indicator for battery performance.

Hence, $LiBF_4$ in pure GBL has very similar performance to conventional electrolytes, and it is important to find optimal electrolyte solvents and/or Li salt composition vs. capacity utilization. For our study, we have chosen only high boiling point cyclic carbonates (EC and PC) as co-solvents for GBL (main component) to preserve and do not scarify its thermal stability with adding low boiling point components. Table 3 presents tested electrolytes to identify the electrolyte composition for optimal battery performances. For this test, MCMB and LNCA electrodes have been used in coin cell as test vehicle and GBL2 electrolyte composition has been chosen as a favorite according to cell performance (not discussed here).

According to the data listed in Table 3, the ionic conductivity of the GBL-based electrolytes is 10–15% lower than most of the conventional electrolytes used in Li-ion batteries. Electrolyte with equal EC/GBL (by volume) amounts and higher salt concentration (Table 3, GBL1) showed conductivity value about 6.14 $mScm^{-1}$. This is probably a result that the affinity between the lithium ion and GBL is very strong and this solvation is reasonably independent of both the anion and salt concentration as have been shown by Aihara et al. [26] using pulsed gradient spin-echo nuclear magnetic resonance. Addition of a small amount of PC, however, will slightly decrease ionic conductivity, which is probably due to a different solvation ability of the GBL and EC/PC molecules as discussed above.

Electrolyte/separator affinity and McMullin number

Microporous polyolefin separator is one of the major components of the Li-ion battery and used to prevent electronic contact and for safety aspects as well to allow ion transport between the positive and negative electrodes. Most of the separator films are made from

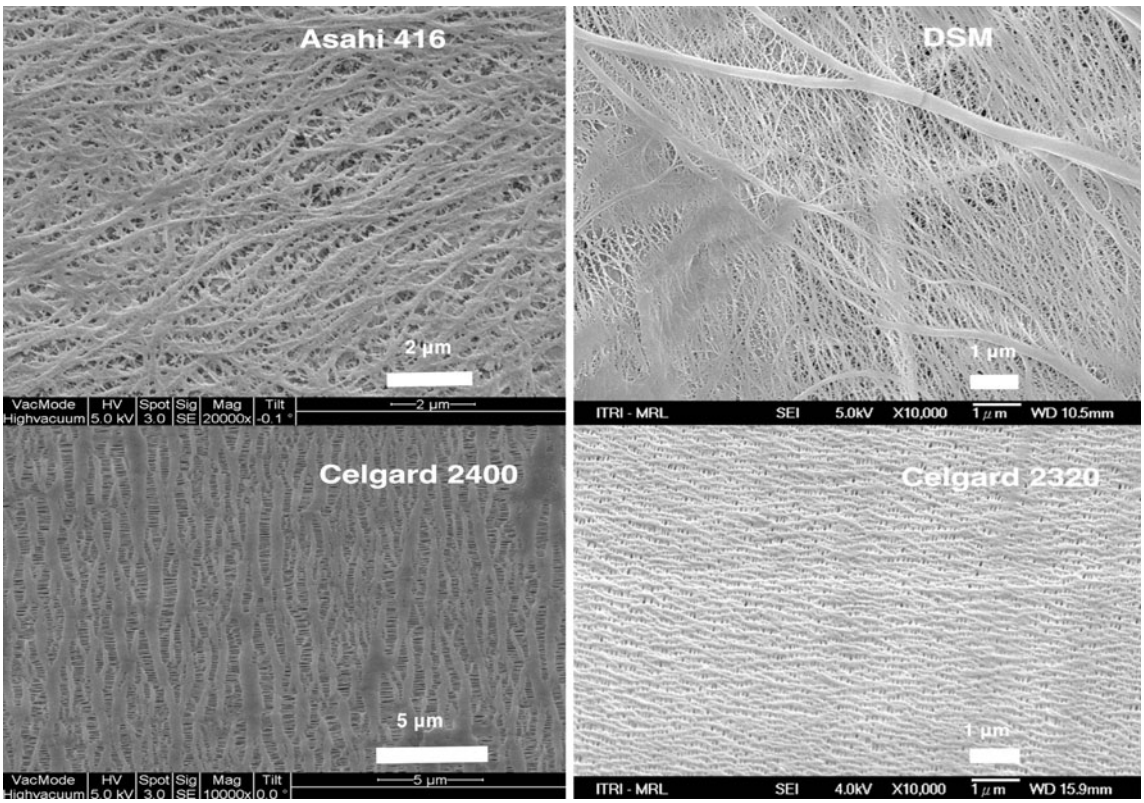

Fig. 8 SEM micrographs of DSM, Asahi, Celgard 2320, and Celgard 2400 separator surface morphology

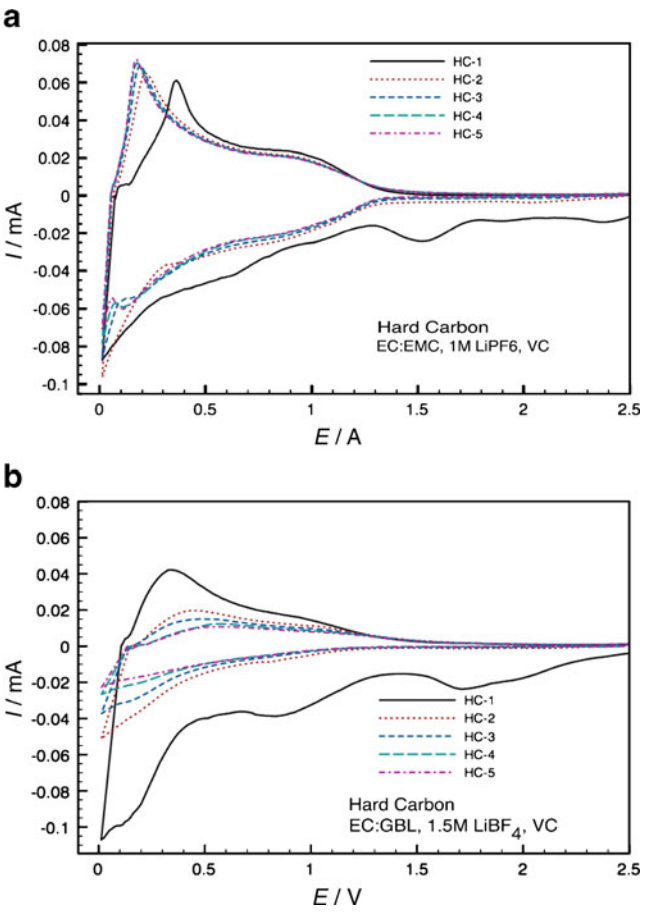

Fig. 9 **a** CV curves of hard carbon/Li half cell with EC/EMC, 1:2, 1 M $LiPF_6$. **b** CV curves of hard carbon /Li half cell with EC/GBL, 1:1, 1.5 M $LiBF_4$

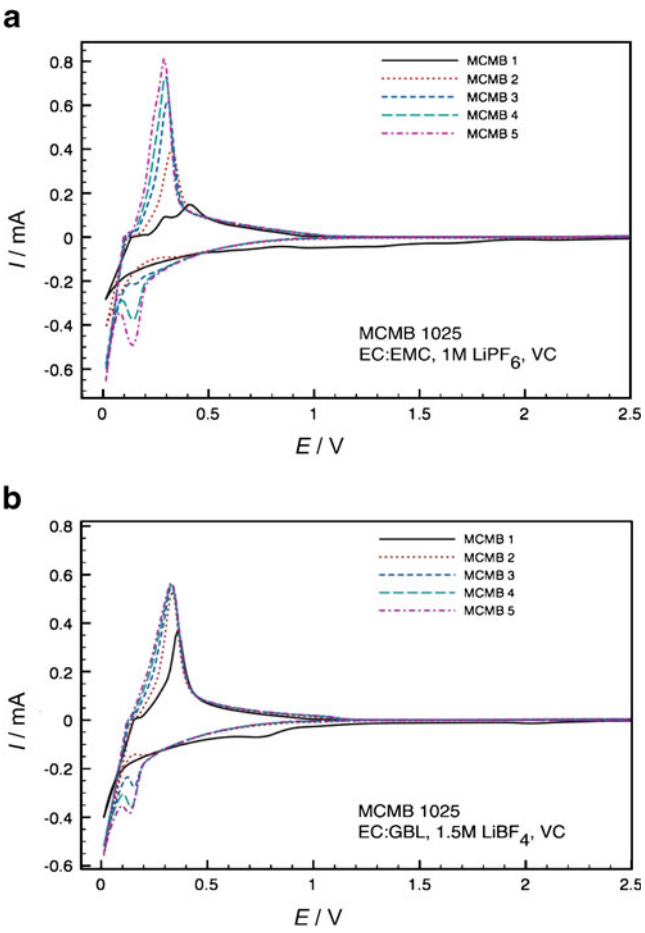

Fig. 10 **a** CV curves of MCMB1028/Li half cell with EC/EMC, 1:2, 1 M $LiPF_6$. **b** CV curves of MCMB1028/Li half cell with EC/GBL, 1:1, 1.5 M $LiBF_4$

polyethylene, polypropylene, or a combination of polyethylene with polypropylene to increase mechanical and thermal properties of thin membrane (thickness in the range from 16 to 25 μm). The properties (mechanical strength, porosity, and wet ability to electrolyte) of the separators made by wet or dry techniques may be quite different. However, all of them have low surface energy and its wet ability by polar organic solvents such as EC, PC, and GBL is in the range from extremely weak to none. Therefore, it will block ion transport, which leads to cycling inability. This is one of the main drawbacks of using a polyolefin membrane in a Li-ion battery. Also, by modifying (a) the surface tension of the separator film by corona (plasma) treatment (which may destroy polyolefin structure and will negatively affect battery calendar life and safety) or (b) the electrolyte solution by an introduction of a small amount of a surfactant agent (no mention of using non-cyclic solvents), it is possible to overcome this problem. We have tested the ionic conductivity of the several separator films with a GBL-based electrolyte and non-ion surfactant in comparison with the reference EC/EMC electrolyte. The results for different types of separators are demonstrated in Table 1.

There is no obvious correlation between separator thickness, porosity, and McMullin number among those data. However, in case when GBL-based electrolyte is used, the McMullin number increased in the following order: Asahi > Celgard 2320 > Celgard 2400 > DSM. This order correlated only with separator thickness in the first three lines of Table 1, and DSM is an exception. For EC/EMC electrolyte, there is no correlation for those data. McMullin number of the DSM separator is the highest among four separators for both electrolyte types in this test in spite of its wet ability which is much better than other samples (estimated by impregnation rate in Table 1). Such a random behavior of the separators may be explained by different morphology (Fig. 8), pore size, and tortuosity. The interesting and useful finding here is that GBL-based electrolyte shows a relatively better McMullin number

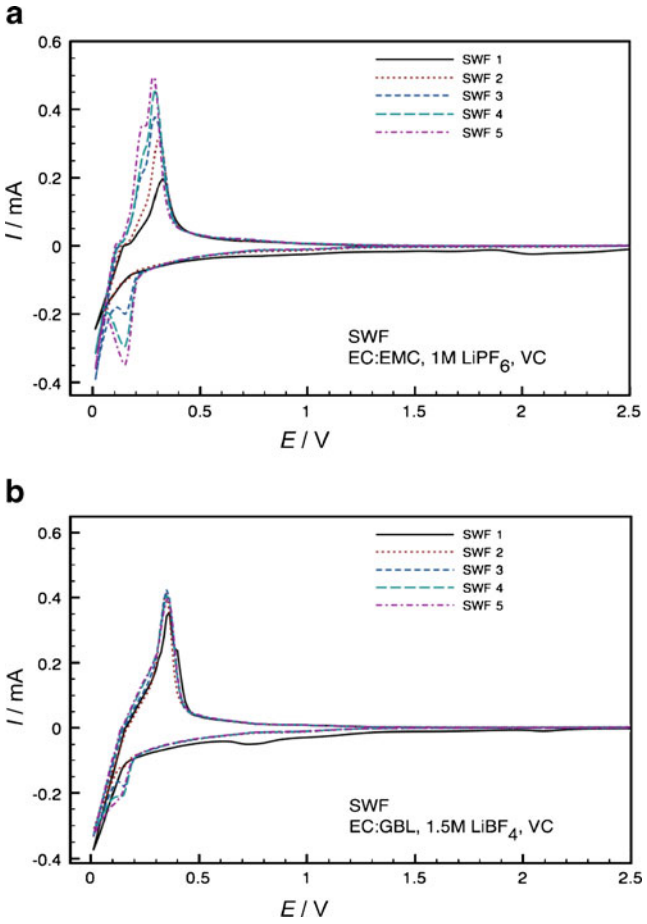

Fig. 11 **a** CV curves of SWF/Li half cell with EC/EMC, 1:2, 1 M $LiPF_6$. **b** CV curves of SWF/Li half cell with EC/GBL, 1:1, 1.5 M $LiBF_4$

compared with reference (EC/EMC) electrolyte, although its ionic conductivity is not that high. In further electrochemical tests, we have used GBL-based electrolyte with surfactant.

Cyclic voltammetry—negative electrode

Cyclic voltammetry (CV) study has been performed in order to obtain information on the influence of the GBL-based electrolyte on active material behavior such as effectiveness of the SEI layer. CV tests of half cells (MCMB1028, SWF, and hard carbon vs. Li/Li^+) in GBL1 and EC/EMC electrolytes have been performed at a slow sweep rate of 0.05 mV s^{-1} between 2.5 and 0.01 V and shown in Figs. 9, 10, and 11. Motivation to use GBL1 vs. GBL2 (with 10% PC), which actually shows better performance, is to simplify SEI creation process and data analysis in this study. All electrolyte compositions included 2 wt.% of VC (Table 3). VC is a "de facto" necessary component of the electrolyte for Li-ion battery as an effective additive for SEI (mainly on the anode) [27].

CV of the hard carbon The first five cycles of the half cell with hard carbon and EC/EMC and GBL1 electrolytes are shown in Fig. 9a, b. It indicates that intercalation/deintercalation of Li^+ in hard carbon mainly occurs in the wide range of potentials (0.01–1.0 V). CV curves of hard carbon do not demonstrate clear peaks after the first cycle, which normally corresponds to the insertion or extraction of Li ions. For the cell with EC/EMC electrolyte (Fig. 9a) at the first cycle, we can observe two obvious reductive peaks appearing at 2.4 and 1.5 V and a small peak at around 0.6 V. The first cycle for the cell with the GBL1 electrolyte (Fig. 9b) shows two broad reductive peaks at 1.7–2 V and 0.8–0.9 V. The peaks for both electrolytes are quite different and may be a consequence of various electrolyte reactions on the very active surface of hard carbon. However, in case of the EC/EMC electrolyte, hard carbon electrode shows good reversibility of Li intercalation/deintercalation. On the contrary, the sample with GBL1 shows poor cycle ability and capacity (Fig. 9b) due to thick passivation film created on the carbon surface which can be seen on the SEM photograph of the cycled electrode (Fig. 13c).

CV of the MCMB The first cycle of the second sample, MCMB/Li cell in EC/EMC electrolyte (Fig. 10a), shows a broad but a small reductive peak from 1.9 to 0.9 V with an increasing capacity during the next cycling (oxidative peak). Cell of MCMB/Li with GBL1 electrolyte reveals a peak at 0.75 V and good reversibility during all five cycles (oxidative peak).

CV of the SWF The third sample, SWF/Li with EMC (Fig. 11a) and GBL1 (Fig. 11b) electrolytes, shows a quite

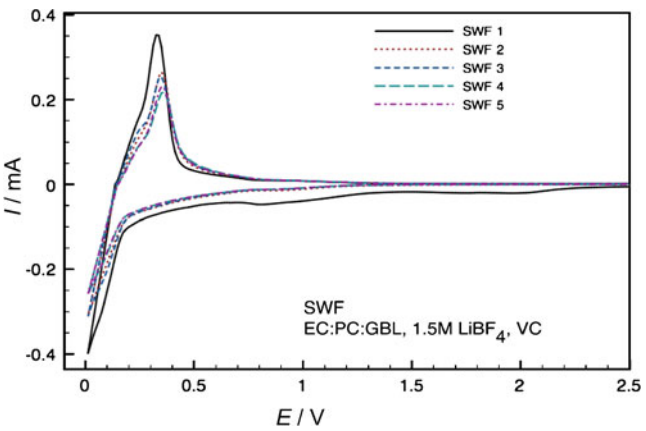

Fig. 12 CV curves of SWF/Li half cell with EC/PC/GBL, 1.4 M $LiBF_4$

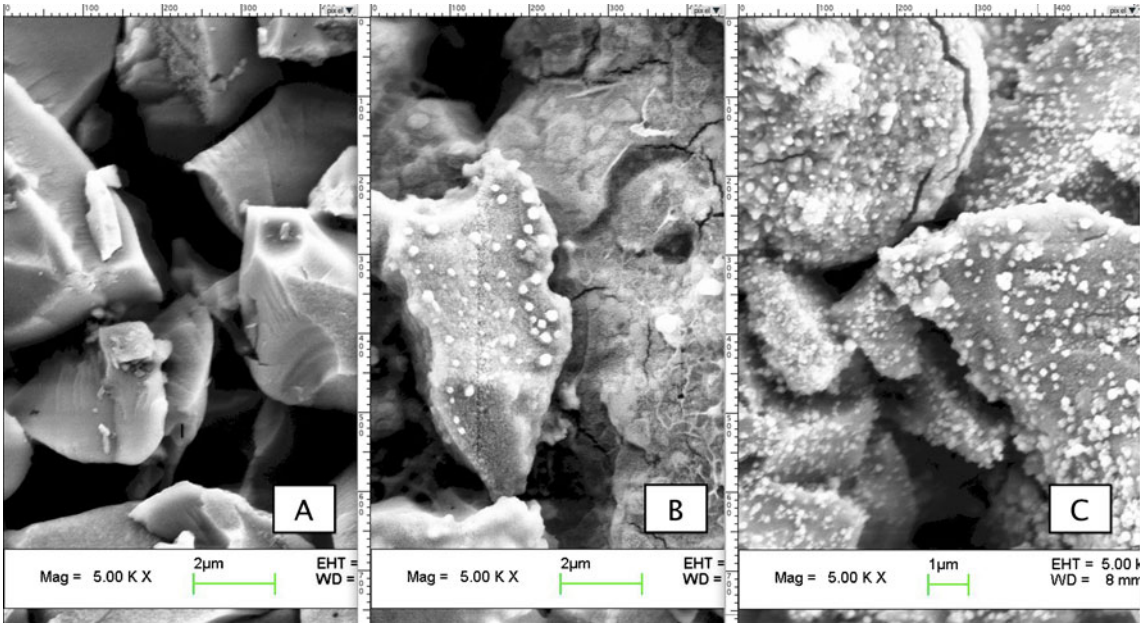

Fig. 13 SEM of negative electrodes (hard carbon) before (**a**) and after cycle in EC/EMC (**b**) and EC/GBL (**c**) electrolyte

similar behavior to each other and to the sample with MCMB electrode with totally reflecting reductive peak at 0.75 V. Sample with EC/EMC electrolyte indicates sharp peaks below 0.3 V (reversible Li intercalation).

In addition, Fig. 12 shows the CV curve of the SWF/Li cell with 10 wt.% of PC added to the GBL-based electrolyte (composition GBL2, Table 3). There are two mostly significant differences in the CV profile as compared with samples without PC (Fig. 10). The first reduction peak that appeared in the previous tests (SWF and MCMB) becomes broader and its maximum shifted from 0.75 V to 0.85 V, and the second peak below 0.3 V disappeared. Thus, even after the addition of 10 vol.% of PC the cycle ability remains the same as for PC-free composition.

These experiments revealed that the GBL-based electrolyte has quite similar Li reversibility compared to EC/EMC-based electrolyte at least for MCMB and SWF negative electrodes, and can form a stable SEI layer at the first cycle. In case of use hard carbon as a negative electrode, the process of the SEI formation and Li intercalation/deintercalation is more complicated for both electrolyte types (GBL-based and reference) and probably related to its surface chemistry. Samples with GBL1 electrolyte show an irreversible peak at about 0.75–0.85 V that is possible to assign to the more complex GBL decomposition process [28].

SEM of negative electrode after cycle

The basic difference in behavior of the negative electrode (hard carbon) in the CV test may be explained by formation of a different quality of SEI layer on the electrode surface. The SEM images of the hard carbon surface before and after five cycles at 1 C current and room temperature are shown on Fig. 13a–c and revealed obvious differences in the surface film quality. The surface film on the hard carbon electrode formed by EC/EMC electrolyte looks more dense and thinner as can be seen on the cracked part (Fig. 13b) in comparison to the surface film on the same electrode formed by the GBL-based electrolyte (Fig. 13c).

For further tests, we exclude hard carbon from our study and assembled full cells in configuration as: SWF/DSM/LNCA in an Al-laminated bag (prismatic jellyroll) cells with design capacity at 375 mAh. The choice to use the DSM separator for this test over others with lower McMullin number is due to its better wet ability to GBL-based electrolyte, which is important when a full cell is constructed.

Impedance data: three-electrode cell study

The three-electrode test cell with Li metal strip (2× 20 mm) as a reference electrode to determine the electrolyte effect on both positive and negative electrodes during SEI formation and after the cycle test has been assembled in an Al-laminated bag (jellyroll prismatic) cell. Cycle tests of the cells containing EC/EMC and GBL1 electrolytes were conducted at room temperature. Figure 14a–c shows EIS impedance spectra of the full cell, and NE and PE after formation procedure at 4.2 V, respectively.

The first semicircle on the Nyquist plot may be attributed to surface film impedance, which corresponds

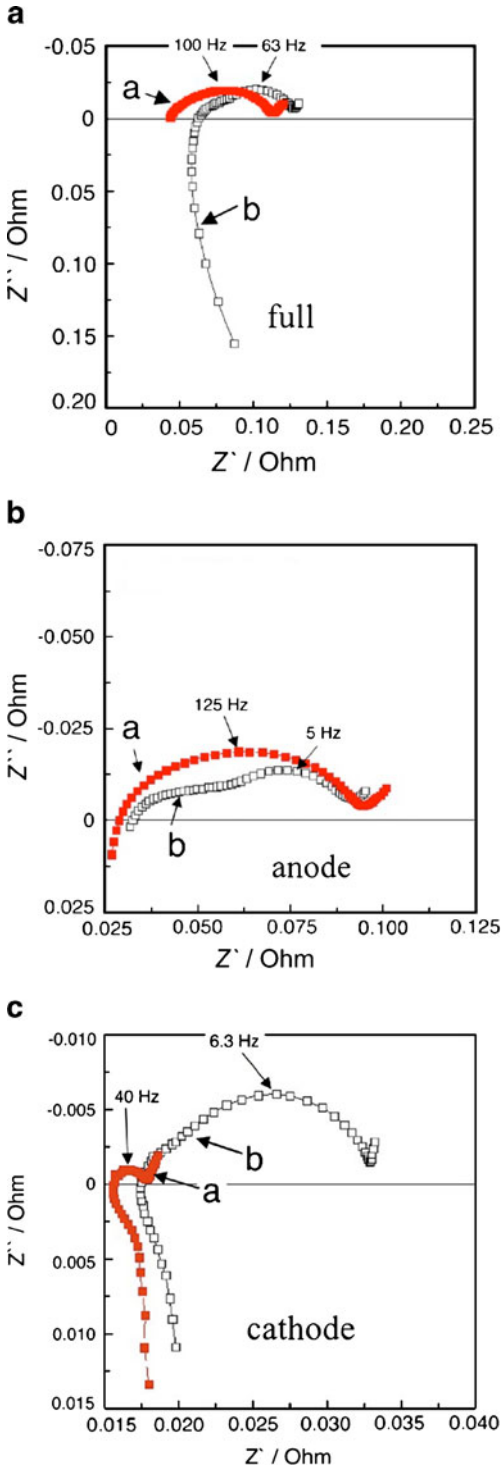

Fig. 14 **a–c** EIS data of (1) full cell, (2) cathode, and (3) anode after formation (C/5, RT); SWF/DSM/LNCA (375 mAh) with *a* EC/GBL and *b* EC/EMC electrolytes and Li metal reference electrode. Data acquired at 4.2 V

to the Li^+ ion's migration through SEI, and the second semicircle as the charge transfer and low frequency tail (45° slope) reflects the diffusion process. Interestingly, that samples with EC/EMC (marked as "b") electrolyte always has two well–pronounced semicircles while samples with the GBL-based electrolyte (marked as "a") show well-

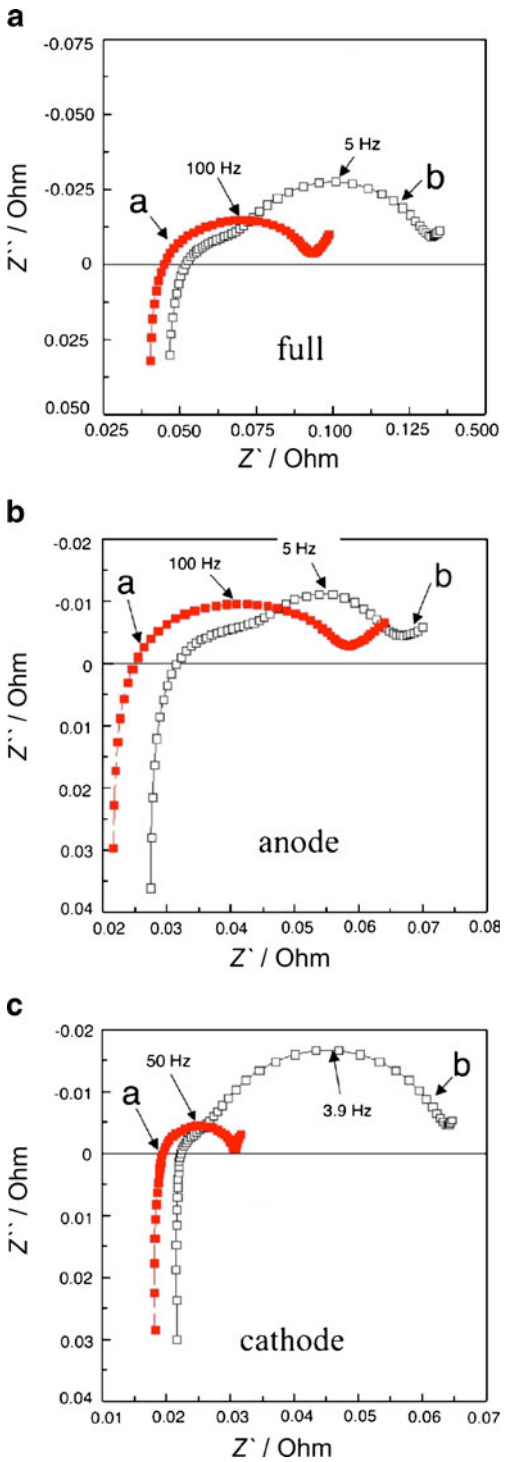

Fig. 15 **a–c** EIS data of (1) full cell, (2) cathode, and (3) anode after 50 cycles (1 C/1 C; RT) of the full cell SWF/DSM/LNCA (375 mAh) with *a* EC/GBL and *b* EC/EMC electrolytes and Li metal reference electrode. Data acquired at 4.2 V

Table 4 Frequency data of AC impedance test (f_w—Warburg tail) for the negative, positive electrodes and full cell as a function of electrolyte type

Electrolyte	Negative f_w	Positive f_w	Full cell f_w
After formation			
EC/EMC	1.25	0.31	0.25
GBL1	0.3	2.5	1.2
After 50 cycles			
EC/EMC	0.31	1.25	0.25
GBL1	1.25	0.2	1.2

formed single semicircle either full cell resistance or separated anode/cathode electrodes. After the first cycle, i.e., SEI formation, anode electrode resistance is almost identical in both samples. On the other hand, the resistance of the cathode electrodes indicates a significant difference where resistance for GBL-based electrolytes is smallest. This may be due to the thickness and/or density difference of the SEI films created on the cathode electrode in different electrolytes. In turn, a difference in the SEI film thickness and/or density on the cathode and their resistivity was determined by greater GBL-based electrolyte's electrochemical stability [29].

The Nyquist plot in Fig. 15a–c demonstrates EIS test data of the full cell and separate anode/cathode for cells with EC/EMC and GBL1 electrolytes after 50 cycles. There is not much variation for the anode side in both electrolytes (Fig. 15a). However, resistance of the cathode electrode cycled in EC/EMC electrolyte (Fig. 15b) is notably increased, which reflect to the full cell profile correspondingly (Fig. 15c and Table 4).

Figure 16a, b demonstrates the cycle test of the full cells with two types of electrolyte (EC/EMC, GBL2) at room (a) and elevated (b) temperatures. Cell with the GBL-based electrolyte shows a slightly higher capacity during a high temperature test. In general, there is no significant contrast in cycle behavior for those two types of electrolytes.

Conclusion

Electrolyte solution EC/(PC)/GBL with $LiBF_4$ has been used for studying its thermal stability by DSC and ARC tests in comparison with EC/EMC ($LiPF_6$). ARC test of the GBL-based electrolytes shows that it is stable up to 350 °C because of lower vapor pressure and high flash point compared to electrolytes with linear carbonates. Electrochemical performances of GBL-based electrolytes have been studied with different negative electrode materials (MCMB, SWF, hard carbon) and compared with reference electrolyte (EC/EMC). It was shown that the GBL-based electrolyte has a compatible cycle ability with most negative materials. An EIS study of the three-electrode technique shows that the GBL-based electrolyte shows much lower impedance on a positive electrode and equal or lower on negative even after prolonged cycling. Possible application of the GBL-based electrolytes, in general, is limited by its low or non-wet ability with common PO separators. Addition of the small amount of suitable surfactant or using non-woven separator will simplify employment of GBL-based electrolytes in Li-ion batteries. To obtain a reliable test result, the McMullin number must be taken as a main index of GBL-based electrolyte affinity to PO separator.

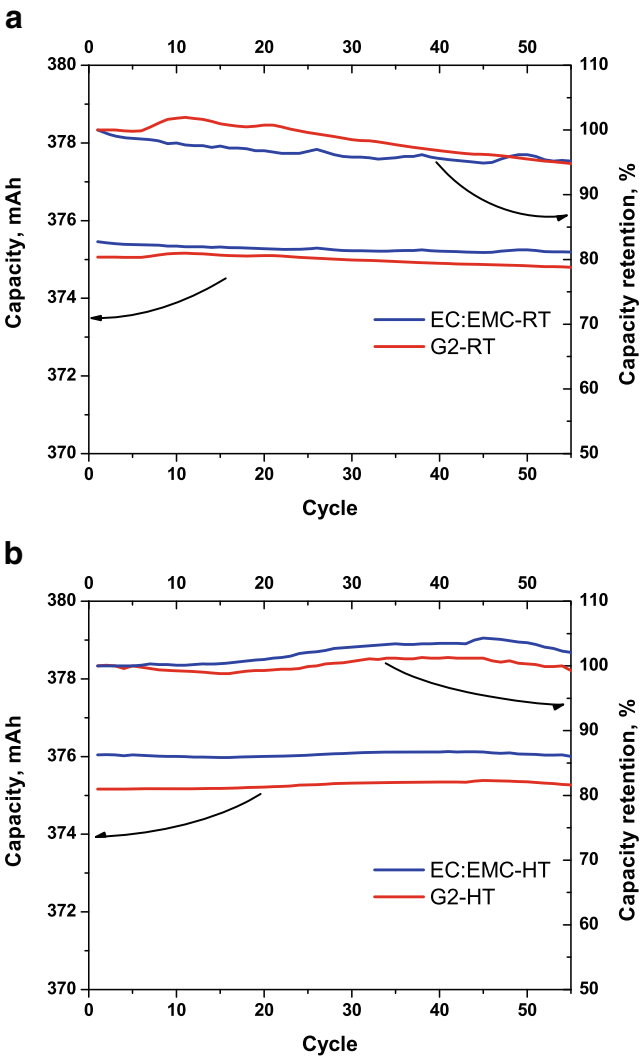

Fig. 16 Cycle test of the Al pouch bag cell (375 mAh), SWF/LNCA with EC/EMC and EC/PC/GBL (G2) electrolytes, **a** at room (25 °C) (RT) and **b** high (55 °C) temperature (HT)

References

1. Shigematsu Y, S-i K, Ue M (2006) Thermal behavior of a C/$LiCoO_2$ cell, its components, and their combinations and the effects of electrolyte additives. J Electrochem Soc 153(11):A2166
2. Kumaresan K, Sikha G, White RE (2008) Thermal model for a Li-ion cell. J Electrochem Soc 155:A164
3. Hatchard TD, MacNeil DD, Basu A, Dahn JR (2001) Thermal model of cylindrical and prismatic lithium-ion cells. J Electrochem Soc 148:A755
4. Belov D, Yang M-H (2008) Investigation of the kinetic mechanism in overcharge process for Li-ion battery. Solid State Ionics 179:1816–1821
5. Zhang S (2006) A review on electrolyte additives for lithium-ion batteries. J Power Sources 162:1379–1394
6. Belov D, Yang M-H (2007) Ineffectiveness of electrolyte additives for overcharge protection in Li-ion battery. ECS Trans 6:29–44
7. Ui K, Yamamoto K, Ishikawa K, Minami T, Takeuchi K, Itagaki M, Watanabe K, Koura N (2008) Development of non-flammable lithium secondary battery with room-temperature ionic liquid electrolyte: performance of electroplated Al film negative electrode. J Power Sources 183:347–350
8. Lewandowski A, Świderska-Mocek A (2009) Ionic liquids as electrolytes for Li-ion batteries—an overview of electrochemical studies. J Power Sources 194:601–609
9. Yang H, Zhuang GV, Ross PN Jr (2006) Thermal stability of LiPF6 salt and Li-ion battery electrolytes containing LiPF6. J Power Sources 161:573–579
10. Ue M (1994) Mobility and ionic association of lithium and quaternary ammonium salts in propylene carbonate and gamma-butyrolactone. J Electrochem Soc 141:3336–3342
11. Zaghib K, Striebel K, Guerfi A, Shim J, Armand M, Gauthier M (2004) $LiFePO_4$/polymer/natural graphite: low cost Li-ion batteries. Electrochim Acta 50:263–270
12. Takami N, Ohsaki T, Hasebe H, Yamamoto M (2002) Laminated thin Li-ion batteries using a liquid electrolyte. J Electrochem Soc 149:A9
13. Lanz M, Novák P (2001) DEMS study of gas evolution at thick graphite electrodes for lithium-ion batteries: the effect of γ-butyrolactone. J Power Sources 102:277–282
14. Morita M (2003) Anodic behavior of aluminum current collector in LiTFSI solutions with different solvent compositions. J Power Sources 119-121:784–788
15. Botte GG, White RE, Zhang Z (2001) Thermal stability of LiPF6-EC:EMC electrolyte for lithium ion batteries. J Power Sources 97-98:570–575
16. Lu Z, Yang L, Guo Y (2006) Thermal behavior and decomposition kinetics of six electrolyte salts by thermal analysis. J Power Sources 156:555–559
17. Hong E-S, Okada S, Sonoda T, Gopukumar S, J-i Y (2004) Thermal stability of electrolytes with mixtures of LiPF6 and LiBF4 used in lithium-ion cells. J Electrochem Soc 151:A1836
18. PTCL safety glossary. Available at http://msds.chem.ox.ac.uk/glossary/nonflammable.html
19. Wang Y, Zaghib K, Guerfi A, Bazito F, Torresi R, Dahn J (2007) Accelerating rate calorimetry studies of the reactions between ionic liquids and charged lithium ion battery electrode materials. Electrochim Acta 52:6346–6352
20. Xu K (2004) Nonaqueous liquid electrolytes for lithium-based rechargeable batteries. Chem Rev 104:4303–4417
21. Chagnes A, Carre B, Willmann P, Dedryvere R, Gonbeau D, Lemordant D (2003) Cycling ability of γ-butyrolactone–ethylene carbonate based electrolytes. J Electrochem Soc 150:A1255
22. Jiang J, Dahn JR (2003) Comparison of the thermal stability of lithiated graphite in LiBOB EC/DEC and in LiPF[sub 6] EC/DEC. Electrochem Solid-State Lett 6:A180–A182
23. Zinigrad E, Larush-Asraf L, Salitra G, Sprecher M, Aurbach D (2007) On the thermal behavior of Li bis(oxalato)borate LiBOB. Thermochim Acta 457:64–69
24. Aihara Y, Arai S, Hayamizu K (2000) Ionic conductivity, DSC and self diffusion coefficients of lithium, anion, polymer, and solvent of polymer gel electrolytes: the structure of the gels and the diffusion mechanism of the ions. Electrochim Acta 45:1321–1326
25. Xu K (2008) Tailoring electrolyte composition for LiBOB. J Electrochem Soc 155:A733
26. Aihara Y, Bando T, Nakagawa H, Yoshida H, Hayamizu K, Akiba E, Price WS (2004) Ion transport properties of six lithium salts dissolved in γ-butyrolactone studied by self-diffusion and ionic conductivity measurements. J Electrochem Soc 151:A119
27. Lee H, Choi S, Kim H, Choi Y, Yoon S, Cho J (2007) SEI layer-forming additives for LiNi0.5Mn1.5O4/graphite 5V Li-ion batteries. Electrochem Commun 9:801–806
28. Aurbach D (1989) Identification of surface films formed on lithium surfaces in gamma-butyrolactone solutions. J Electrochem Soc 136:1606–1610
29. Ding M, Xu K, Zheng JP, Jow TR (2004) γ-Butyrolactone–acetonitrile solution of triethylmethylammonium tetrafluoroborate as an electrolyte for double-layer capacitors. J Power Sources 138:340–350